

## Prodan as a Membrane Surface Fluorescence Probe: Partitioning between Water and Phospholipid Phases

Ewa K. Krasnowska,\* Enrico Gratton,# and Tiziana Parasassi\*

\*Istituto di Medicina Sperimentale, Consiglio Nazionale delle Ricerche, 00137 Rome, Italy, and #Laboratory for Fluorescence Dynamics, University of Illinois at Urbana-Champaign, Urbana, Illinois 61801 USA

**ABSTRACT** Fluorescence spectral features of 6-propionyl-2-dimethylaminonaphthalene (Prodan) in phospholipid vesicles of different phase states are investigated. Like the spectra of 6-lauroyl-2-dimethylaminonaphthalene (Laurdan), the steady-state excitation and emission spectra of Prodan are sensitive to the polarity of the environment, showing a relevant shift due to the dipolar relaxation phenomenon. Because of the different lengths of their acyl residues, the partitioning of the two probes between water and the membrane bilayer differs profoundly. To account for the contribution of Prodan fluorescence arising from water, we introduce a three-wavelength generalized polarization method that makes it possible to separate the spectral properties of Prodan in the lipid phase and in water, and to determine the probe partitioning between phospholipid and water and between the gel and the liquid-crystalline phases of phospholipids. In contrast to Laurdan, Prodan preferentially partitions in the liquid-crystalline phase with respect to the gel and is sensitive to the polar head pretransition, and its partition coefficient between the membrane and water depends on the phase state, i.e., on the packing of the bilayer. Prodan is sensitive to polarity variations occurring closer to the bilayer surface than those detected by Laurdan.

### INTRODUCTION

Bilayer polarity is the subject of current investigations of model and natural membranes (Stubbs et al., 1995). The polarity properties of the membrane bilayer are strongly influenced by its composition and dynamics (Damodaran and Kenneth, 1994). The phospholipid phase transition (gel to liquid-crystalline) profoundly affects the bilayer water content (Heller et al., 1993; Chiu et al., 1995; Parasassi and Gratton, 1995; Parasassi et al., 1997). Similarly, it has been proposed that ordered microdomains locally modify the membrane polarity. For instance, in one- and two-component phospholipid bilayers, the introduction of guest molecules such as pyrene-PC (Tang and Chong, 1992) or cholesterol (Virtanen et al., 1995; Parasassi et al., 1994a) strongly modifies the phospholipid dynamical properties and, at peculiar concentrations, may also induce ordered molecular microdomains. Furthermore, lipid oxidation processes lead to the formation of hydrophilic residues in the bilayer core, which favor the penetration of water (Parasassi et al., 1994b).

Many membrane fluorescent probes are sensitive to bilayer polarity. The fluorescence decay kinetics of several membrane probes depend on the dielectric constant of their environment (Stubbs et al., 1995; MacGregor and Weber, 1981). Particularly attractive are those probes with environmentally sensitive steady-state fluorescence parameters (MacGregor and Weber, 1981; Slavik, 1982; Lakowicz et

al., 1983; Parasassi et al., 1994b). Among the spectral sensitive probes are 6-propionyl- and 6-lauroyl-2-dimethylaminonaphthalene, Prodan and Laurdan, respectively, first introduced by Gregorio Weber (Weber and Farris, 1979; MacGregor and Weber, 1981). A noticeable redshift of their emission is observed with increasing solvent polarity (Massey et al., 1985; Chong, 1988; Zeng and Chong, 1991; Rottenberg, 1992; Parasassi et al., 1994b; Bondar and Rowe, 1996), because of the dipolar relaxation phenomenon (MacGregor and Weber, 1981). The generalized polarization (GP) method was developed (Parasassi et al., 1990) to quantitatively analyze the differences in the emission spectra, and to exploit a possible selective excitation of two probe populations in different environments. The advantages of the GP method reside in its sensitivity to the properties of the membrane (Parasassi et al., 1994b) and in the possibility of determining and quantifying the phase state of the membrane (Parasassi et al., 1993).

The variation in Laurdan fluorescence parameters as a function of the phospholipid composition and of cholesterol concentration has been characterized in detail (Parasassi and Gratton, 1995). The comparison between Laurdan and Prodan behavior has been utilized to clarify the molecular origin of variations in membrane dynamics as a function of oxidative damage (Parasassi et al., 1994b). Because of the different lengths of their acyl residues, the two probes locate differently in the bilayer depth, and their affinities for the membrane and the different phase domains in the membrane may profoundly differ. Therefore, modification of the membrane polarity due, for instance, to phase transitions, can also cause the relocation of the fluorescent probes in bilayer (Parasassi et al., 1991c) and changes of the probe affinity for the membrane (Zeng and Chong, 1995).

To address this problem, we developed a method to simultaneously measure the environment polarity and the

Received for publication 9 December 1997 and in final form 31 December 1997.

Address reprint requests to Dr. Dr. Tiziana Parasassi, Istituto di Medicina Sperimentale, CNR, Viale Marx 15, 00137 Roma, Italy. Tel.: 39-6-86090.316; Fax: 39-6-86090.332; E-mail: tiziana@biocell.irmkamt.rm.cnr.it.

© 1998 by the Biophysical Society

0006-3495/98/04/1984/10 \$2.00

probe partitioning between the aqueous and lipid environment and its relative amount in the gel and liquid-crystalline phase. Our method is based on a modification of the GP function, utilizing three emission wavelengths rather than two, as we previously did for Laurdan. In the course of this study, we have determined that Prodan partitions between the bilayer and water and that there is a substantial preferential partitioning in the liquid-crystalline phase. With respect to Laurdan, because of its different location in the membrane closer to the aqueous surface of the bilayer, Prodan is also sensitive to the pretransition in the polar head region.

## MATERIALS AND METHODS

Multilamellar phospholipid vesicles were prepared by mixing the appropriate amounts of solutions in chloroform (spectroscopic grade) of phospholipids (dilauroyl- and dipalmitoylphosphatidylcholine, DLPC and DPPC, respectively; Avanti Polar Lipids, Alabaster, AL) and fluorescent probes (6-propionyl and 6-lauroyl-2-dimethylaminonaphthalene, Prodan and Laurdan, respectively; Molecular Probes, Eugene, OR) and then evaporating the solvent by nitrogen flow. The dried samples were resuspended in Dulbecco's phosphate-buffered saline solution, pH 7.4 (PBS) (Sigma Chemical Co., St. Louis, MO), heated above the transition temperature, and vortexed. The samples were then transferred to a cuvette and equilibrated at the desired temperature in the fluorimeter cell holder for 10 min. All samples were prepared in red light and used immediately after preparation. Unless differently specified, the final lipids and probe concentrations were 0.3 mM and 0.3  $\mu$ M, respectively. To subtract the background contribution to the emission, samples of the same phospholipids and at the same concentrations were prepared, omitting the addition of the probes. In the dilution experiments, the sample composed of both the lipids and the probe was diluted by adding the buffer solution.

A modified preparation was used for those samples employed for the calculation of the  $R_{31}$  and  $R_{32}$  values (Eqs. 5 and 7 in the Results). Multilamellar vesicles of each sample were prepared, each at twice the final concentration and without the addition of the probe. A Prodan suspension in PBS was prepared by adding to PBS the proper amount of a Prodan solution in DMSO (labeling buffer). The final concentration of DMSO in the buffer was less than 0.05%. Samples labeled with different probe concentrations were obtained by adding different aliquots of the labeling buffer to the vesicle suspension. When necessary to reach the final constant phospholipid concentration of 0.3 mM, PBS buffer was added to the samples. The samples were then incubated for 30 min at room temperature, in the dark and under mild stirring. Fluorescence steady-state spectra were obtained with a GREG 200 fluorometer (ISS, Champaign, IL) equipped with photon counting electronics (PX01; ISS) and a xenon arc lamp. The spectra were only corrected for the lamp intensity variation. The sample compartment was thermostated by a circulating water bath to within 0.1°C. The GP value was calculated from the emission spectra by

$$GP = \frac{I_g - I_{lc}}{I_g + I_{lc}} \quad (1)$$

where  $I_g$  is the emission intensity at 440 nm and  $I_{lc}$  is the emission intensity at 490 nm for the calculation of excitation GP, and at 410 nm and 340 nm, respectively, for the calculation of emission GP (Parasassi et al., 1990). Monochromator bandpasses were 8 nm. Fluorescence polarization measurements were performed with the GREG 200 fluorometer, with Glan-Thompson polarizers inserted in the excitation and right emission paths.

Fluorescence lifetime measurements were performed with a K2 phase fluorometer (ISS), with a xenon arc lamp as the light source. Excitation was at 360 nm, and emission was observed through a Janos 418 cutoff filter (Janos Technology, Newfane, VT). An additional polarizer was inserted in the excitation light path, with an angle of 35° with respect to the vertical.

A solution of 2,2'-*p*-phenylene-*bis*-(5-phenyl)oxazole (POPOP) in ethanol was used as the reference (lifetime 1.35 ns). During measurements, samples were continuously stirred. The sample compartment was kept at  $25 \pm 0.1^\circ\text{C}$  by a water circulating bath. Phase and modulation data were collected at 10 modulation frequencies, logarithmically spaced in the range of 0.6–150 MHz.

For time-resolved spectra, the emission was observed through a series of seven interference filters, from 420 nm to 540 nm, with 10 nm bandwidth and at 20-nm intervals. Phase and modulation data were acquired at each emission wavelength, using a set of 10 frequencies, logarithmically spaced from 25 to 250 MHz. Data were analyzed using Globals Unlimited software (Laboratory for Fluorescence Dynamics, University of Illinois at Urbana-Champaign).

## RESULTS

### Laurdan and Prodan fluorescence spectra

The spectral sensitivity of Prodan and Laurdan fluorescence excitation and emission spectra to the phase state of phospholipid multilamellar vesicles has been compared in vesicles composed of pure gel, pure liquid-crystalline, and an equimolar mixture of the two phases. In Fig. 1 *A*, Prodan excitation and emission spectra obtained at 25°C in vesicles of DLPC (liquid-crystalline phase), DPPC (gel phase), and an equimolar mixture of the two phospholipids are reported. The excitation spectra are composed of at least two well-

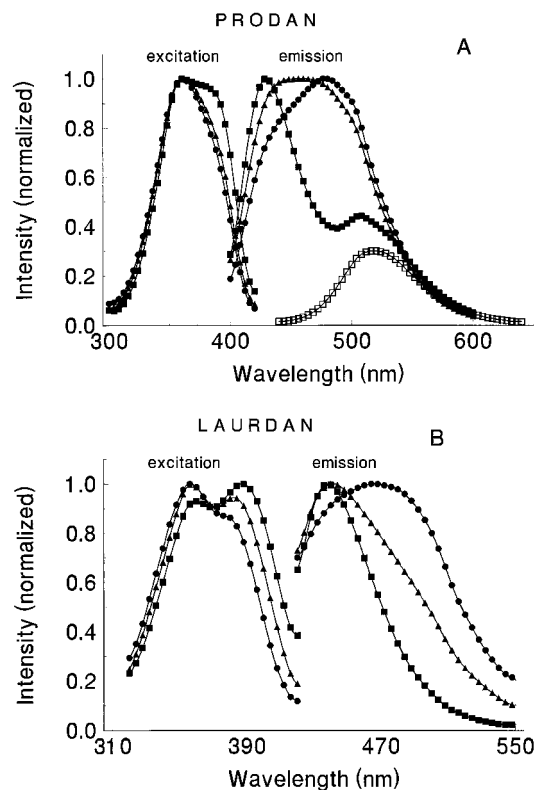


FIGURE 1 Prodan (*A*) and Laurdan (*B*) excitation and emission spectra obtained in multilamellar phospholipid vesicles composed of gel (■, DPPC), liquid-crystalline (●, DLPC), and an equimolar mixture of the two phases (▲, DLPC-DPPC) and (*A*) in water (not normalized) (□) at 25°C. For the excitation spectra the emission wavelength was at  $440 \pm 8$  nm, and for emission spectra the excitation wavelength was at  $360 \pm 8$  nm.

distinguished bands with relative maxima at 360 nm and 390 nm. Prodan intensity variations of the red excitation band in vesicles of different phase states are less pronounced than those of Laurdan (Fig. 1 *B*). In particular, the Prodan excitation spectrum obtained in the equimolar mixture of the two phospholipids is similar to the excitation spectrum obtained in DLPC. With respect to Laurdan emission (maximum emission at 465 nm), we observe a more relevant Prodan emission redshift in the vesicles composed of DLPC (maximum at 477 nm) and the mixture of the two phases (Laurdan maximum at 442 nm and Prodan maximum at 459 nm). The most noticeable difference between Prodan and Laurdan emissions is observed in the spectrum obtained in DPPC with the appearance of an additional emission band centered at  $\sim 520$  nm. This band was later identified as being due to the emission of Prodan molecules in the aqueous phase (Fig. 1 *A*).

### Prodan partitioning in water

Prodan excitation and emission GP spectra, at 25°C, calculated from Eq. 1, are reported in Fig. 2 *A*. In the liquid-crystalline phase (DLPC vesicles), both excitation and emission GP spectra of Prodan show a wavelength dependence similar to that observed using Laurdan (Fig. 2 *B*). In

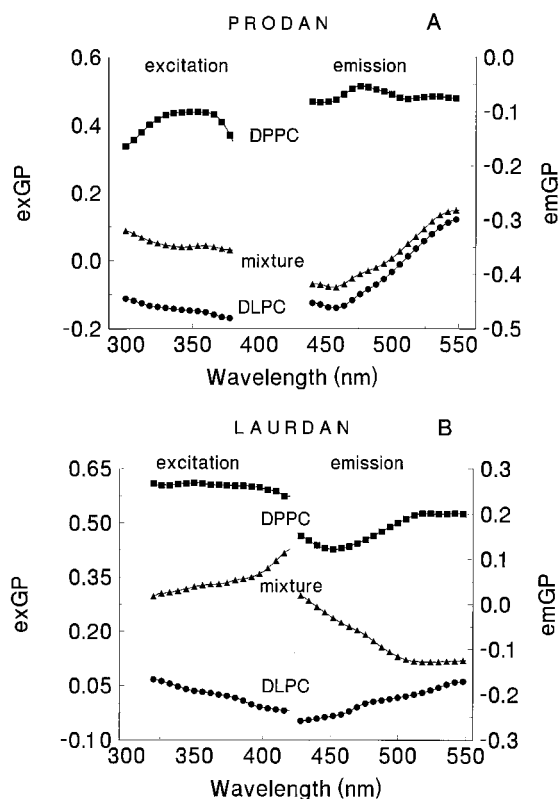


FIGURE 2 Prodan (*A*) and Laurdan (*B*) excitation and emission GP spectra obtained in multilamellar phospholipid vesicles composed of gel (■, DPPC), liquid-crystalline (●, DLPC), and an equimolar mixture of the two phases (▲, DLPC-DPPC) at 25°C. Wavelengths were utilized as in Eq. 1.

DLPC vesicles, Prodan GP value decreases as the excitation wavelengths increase and increases as the emission wavelengths increase. In the DPPC sample, the Prodan excitation GP spectrum shows a composite behavior (Fig. 2 *A*). Instead, no average wavelength dependence is observed in the emission GP spectrum. Contrary to the behavior observed with Laurdan, the Prodan GP spectra obtained in the mixture of the two phases show a wavelength dependence similar to that observed in the DLPC sample, indicating that Prodan may be sensitive only to the liquid-crystalline phase. Prodan GP spectra may indicate a preferential partitioning of the probe in the liquid-crystalline phase with respect to the gel, and, because of the average lower GP value, an appreciable partitioning in water when only the phospholipid gel phase is present. To study the partitioning in the aqueous phase, dilution experiments were performed by adding increasing volumes of the buffer solution. The integrated intensity over the whole emission spectrum is plotted as a function of the final phospholipid (or probe) concentration (for the DPPC sample: Fig. 3 *A*). The average lifetime of Prodan in water is lower than in phospholipids, both in DLPC and in DPPC (Table 1). In the dilution experiments, for all three phospholipid samples, a negative deviation from linearity of the integrated emission was observed (Fig. 3 *B*), indicating that, with dilution, the probe is extracted from the bilayer to the aqueous buffer. In Fig. 3 *A*, to separate the contribution to the total emission of Prodan in water from that of Prodan in DPPC, the integrated emission intensity, from 400 nm to 475 nm, as representative of the probe in DPPC, and from 475 nm to 550 nm, as representative of the probe in water (*inset* of Fig. 3 *A*), was plotted versus phospholipid concentration. The intensity relative to the probe in water (red emission band, from 475 nm to 550 nm) shows a positive deviation from linearity as a function of dilution, indicating that the probe partitions in the buffer. Because of the superposition of the Prodan spectra from the membrane and water, in the liquid-crystalline phase (DLPC vesicles) and in the equimolar mixture of the two phases the emissions of Prodan molecules in water cannot be isolated. Instead, at the concentrations used, Laurdan does not partition in water (Parasassi et al., 1994a; Zeng and Chong, 1995), and for the Laurdan probe we did not observe a deviation from linearity upon dilution (Fig. 3 *B*). Prodan emission spectra as a function of the DPPC concentration are reported in Fig. 4.

The value of Prodan fluorescence polarization has been measured along the emission spectrum in DPPC and in water. The results are reported in Fig. 5. With increasing emission wavelength, Prodan polarization in DPPC shows an abrupt decrease at wavelengths of  $>470$  nm, reaching a value close to that measured in water. A quantitative analysis that accounts for the different intensity of Prodan in the bilayer and in water gives a polarization in agreement with the measured values.

To further verify the origin of the emission band centered at  $\sim 510$  nm, lifetime measurements have been made of the probe in water; in DPPC vesicles at 25°C, using cutoff

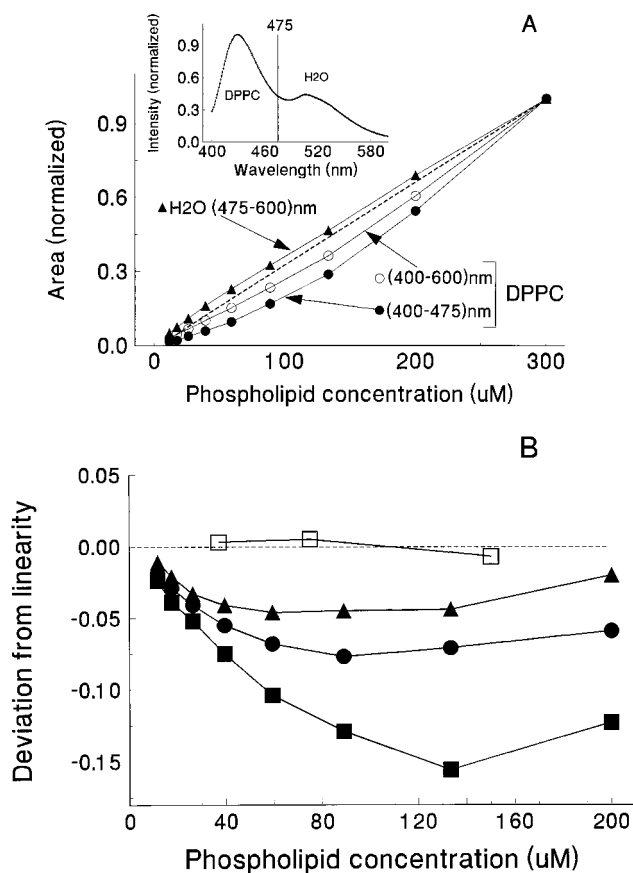


FIGURE 3 (A) Integrated emission intensity of Prodan as a function of the sample concentration in the buffer. Samples of 0.3 mM DPPC and 0.3  $\mu$ M Prodan were progressively diluted by one-third with the buffer; the emission spectra were acquired at 25°C. On the y axis we report the integrated emission intensity of the total emission (from 400 nm to 600 nm;  $\circ$ ), of the emission attributed to the probe in DPPC (from 400 nm to 475 nm;  $\bullet$ ), and of the emission attributed to the probe in water (from 475 nm to 600 nm;  $\blacktriangle$ ), as shown in the inset. The straight dotted line is drawn for comparison. The deviation of the integrated emission from this last dotted line is reported in B, together with the deviation from linearity of the total integrated emission, from 400 nm to 550 nm, of a Laurdan-labeled DPPC sample, progressively diluted by one-half by a procedure similar to that used for the Prodan-labeled sample.

filters that do not transmit below 418 nm and below 470 nm; in DLPC; and in DLPC/DPPC vesicles. The results are summarized in Table 1. Prodan fluorescence decay in DPPC shows two components; the value of the short-lifetime com-

**TABLE 1** PRODAN lifetime values ( $\tau$ ), with the associated width distribution ( $w$ ), in ns, and fractional amplitude ( $f$ ), measured in different phospholipid samples and in water at 25°C

	$\tau_1$	$w_1$	$f_1$	$\tau_2$	$w_2$	$f_2$	$\chi^2$	$\langle\tau\rangle$
DLPC	3.85	—	0.995	0.01	—	0.005	2.12	3.52
DPPC (em > 418)	5.58	—	0.622	1.36	1.85	0.378	3.11	3.98
DPPC (em > 470)	5.43	—	0.410	1.26	1.64	0.590	1.89	2.97
DLPC:DPPC = 1:1	3.89	0.58	0.991	0.01	—	0.009	3.37	3.54
Water	1.41	1.94	1.00	—	—	—	3.07	1.41

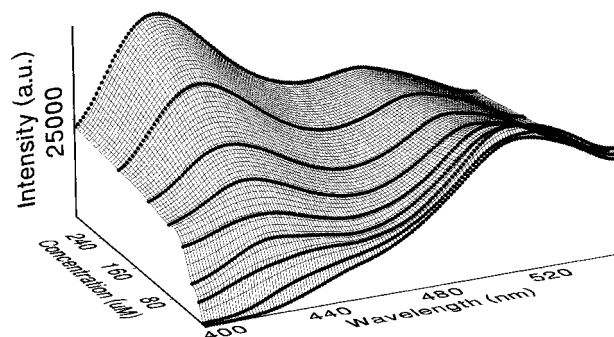


FIGURE 4 Prodan emission spectra in DPPC vesicles at different phospholipid concentrations. The total emission intensity has been normalized to the highest phospholipid concentration. A sample dilution was performed as described in the legend of Fig. 3.

ponent is similar to that determined for the probe in water. In DPPC, as the cutoff filter wavelength increases from 418 nm to 470 nm, the fractional intensity of the short component increases (Table 1). In the other phospholipid samples, at 25°C, a short component of the decay is also present, both with very short lifetime value and very low fractional intensity (less than 0.01).

### Three-wavelength GP value

To subtract the fluorescence emission of Prodan in water and to obtain a GP value for the probe in the bilayer, a three-wavelength excitation GP method (3wGP) was developed by measuring the emission intensity at three wavelengths, chosen to maximize the separation of the contributions from the different Prodan environments (Fig. 6),  $I_1 = 420$  nm,  $I_2 = 480$  nm,  $I_3 = 530$  nm:

$$3wGP = \frac{R_{12} - 1}{R_{12} + 1} \quad (2)$$

where

$$R_{12} = \frac{I_1 k_{32}}{I_2 k_{32} - I_3 + I_3 R_{31}} \quad (3)$$

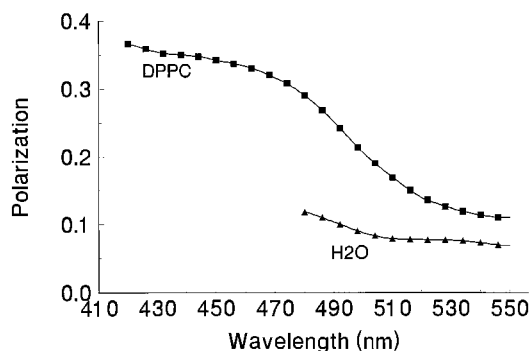


FIGURE 5 Prodan emission polarization spectrum in DPPC vesicles ( $\blacksquare$ ) and in water ( $\blacktriangle$ ) at 10°C.

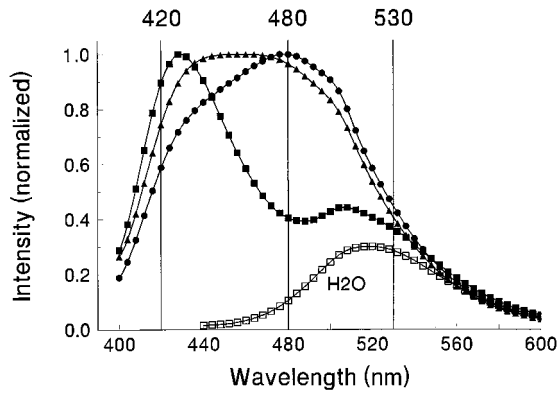


FIGURE 6 Normalized Prodan emission spectra in phospholipid vesicles of the different phase states, as in Fig. 1 *A*. The emission wavelengths used for the calculation of the 3wGP are indicated.

with

$$k_{32} = (I_{3W})/(I_{2W}) \quad (4)$$

$$R_{31} = I_{3M}/I_{1M} \quad (5)$$

where  $I_{1W}$  and  $I_{3W}$  are the emission intensities at 420 nm and 530 nm, respectively, of Prodan in water, separately measured in a sample of Prodan in water, which gave  $k_{32} = 2.8$ ;  $I_{1M}$  and  $I_{3M}$  are the components of the intensities at 420 nm and 530 nm, due only to the probe emission in the membrane after the subtraction of the intensity arising from the probe in water. The  $k_{32}$  value has been measured only once, because we assume that the spectrum of Prodan in water does not change with the kind of phospholipid used. The 3wGP method also allows the measurement of the ratio between Prodan fluorescence arising from the membrane and from the aqueous phase, by using the intensities  $I_2$  and  $I_3$  and the  $k_{32} = 2.8$  value:

$$R_F = \frac{F_M}{F_H} = \frac{I_2 k_{32} - I_3}{I_3 - I_2 R_{32}} \quad (6)$$

where  $F_M$  and  $F_H$  are Prodan fluorescence fractional intensity in the membrane and in water, respectively, and

$$R_{32} = I_{3M}/I_{2M} \quad (7)$$

with  $I_{2M}$  and  $I_{3M}$  representing the component of the intensities at 480 nm and 530 nm, due only to the probe emission in the membrane after subtraction of the intensity arising from the probe in water. Assuming that the lifetime is proportional to the quantum yield, by using the measured values of the probe lifetime in water,  $\tau_W$ , and in the membrane,  $\tau_M$ , a quantitative determination of the ratio between Prodan molecules in the two environments,  $R_M$ , can be achieved:

$$R_M = R_F \frac{\tau_W}{\tau_M} \quad (8)$$

Assuming that the density of the phospholipid bilayer is approximately the same as the water density (Nagle and

Wilkinson, 1978), and following Huang and Haugland (1991), the probe partition coefficient,  $C_p$ , between the bilayer and water can be directly determined if the phospholipid concentration is known:

$$C_p = R_M \frac{[H_2O]}{[\text{lipids}]} \quad (9)$$

Note that Eqs. 2–6 are not simply the solutions of a system of three equations in three unknowns. In fact, the Prodan emission in the liquid-crystalline phase depends on the extent of dipolar relaxation. The emission spectrum moves to the red as a function of time, so that a “standard” spectrum for the relaxed molecules cannot be defined. Therefore, to maintain the GP concept, which measures the extent of the relaxation, we measure the ratio between two wavelengths independently of the water concentration. Equations 2–6 are the “corrections” to this ratio and give the GP value in the presence of Prodan in water.

Equations 3 and 6 contain all directly measured quantities, except for  $R_{31}$  in Eq. 3 and  $R_{32}$  in Eq. 6. We note that in Eq. 3, if  $R_{31} \ll 1$ , then the error in the evaluation of this term has a small effect on the 3wGP value. Because  $R_{31}$  is the ratio between Prodan emissions at 530 nm and 420 nm, in the gel phase this ratio will always be  $\ll 1$ . However, in the liquid-crystalline phase this ratio cannot be larger than 0.7 (Fig. 6). Using the largest possible value, we estimate that the maximum correction to the 3wGP is  $\sim 3\%$ . Instead, the evaluation of the ratio  $R_{32}$  may significantly alter the  $R_F$  value in Eq. 6. Equation 6 can be written as

$$R_F = \frac{I_2 k_{32}}{I_3 - I_2 (I_{3M}/I_{2M})} = \frac{2.8}{(I_3/I_2) - (I_{3M}/I_{2M})} \cong \frac{2.8 \times I_2}{I_3 - I_{3M}} \quad (10)$$

In the last term of Eq. 10, we assume that at 480 nm the contribution of the probe emission in water is small compared to its emission in the membrane, i.e.,  $I_2 \cong I_{2M}$ . Although  $I_{3M}$  is relatively easy to evaluate in the gel phase, it can be more difficult to evaluate in the liquid-crystalline phase, and it can also be equal to  $I_3$ . To separate the contribution of the probe emissions in water and in the membrane in the liquid-crystalline phase at 530 nm, we used the procedure of sample preparation reported in Materials and Methods. Different samples composed of vesicles of each phospholipid were prepared at the constant concentration of 0.3 mM and with variable concentrations of Prodan. The phospholipid:probe ratio was varied between 4000 and 1000. Different percentages of the emission spectrum of Prodan in the labeling buffer were subtracted from the emission of the samples, after blank subtraction, to get overlapping (normalized) spectra. These spectra, representing Prodan emission only from the membrane, at 25°C, have been used for the calculation of the  $R_{31}$  and  $R_{32}$  values. The obtained  $R_{31}$  values were 0.081, 0.394, and 0.700 in DPPC, DPPC/DLPC = 1:1, and DLPC, respectively. The obtained  $R_{32}$  values were 0.293, 0.329, and 0.405 in DPPC, DPPC/DLPC = 1:1, and DLPC, respectively. These values are temperature dependent, particularly in the liquid-crys-

talline phase. To estimate the variation of the  $R_{32}$  value as a function of temperature in the liquid-crystalline phase, we calculated the  $R_{32}$  value of Laurdan-labeled DLPC vesicles, with the assumption that in the case of Laurdan, all of the emission originates from the probe inserted in the membrane.

The 3wGP equations can be simplified by assuming that at 530 nm the contribution to the total emission intensity of Prodan molecules in the membrane is negligible, i.e.,  $I_{3M} = 0$ . We then obtain

$$R_{12} = \frac{I_1 k_{32}}{I_2 k_{32} - I_3} \quad (11)$$

$$R_M = R_F \frac{\tau_W}{\tau_M} = \left( \frac{I_2 k_{32}}{I_3} - 1 \right) \frac{\tau_W}{\tau_M} \quad (12)$$

In this case we obtain a lower bound for the partition coefficient value. The results presented in the following paragraphs have been obtained by using both the simplified Eqs. 11 and 12 and the corrected Eqs. 3 and 6, with the evaluation of the  $R_{32}$  value as previously discussed.

### Temperature dependence of the GP value

The two- and three-wavelength GP values of DPPC vesicles labeled with Prodan or Laurdan are reported in Fig. 7. Using the 3wGP, the phase transition at 41.5°C is more evident. In addition, the 3wGP clearly shows the phospholipid polar head pretransition at temperatures greater than or equal to 30°C. The 3wGP was calculated using both Eqs. 3 and 11. As predicted, the difference between the obtained values is small (Fig. 7 B and Table 2).

In Fig. 8, the temperature variation of the  $R_M$  value (ratio between Prodan molecules in the phospholipid phase and in water), calculated assuming constant lifetimes over the whole temperature range (values in Table 1), is shown. In Fig. 8 A the  $R_M$  lower bound values, calculated with Eq. 12, are reported. In Fig. 8 B, the “corrected”  $R_M$  values, calculated with Eqs. 6 and 8, are reported, using  $R_{32}$  values calculated at 25°C (*open symbols*), and using the estimated temperature variation of  $R_{32}$ , as described above (*filled symbols*). We observe that, in general, the  $R_M$  value strongly depends on the lipid phase state. Noticeably, in the DPPC sample the partition in the lipid phase increases with temperature, showing an abrupt variation with the phospholipid phase transition. This increase in Prodan partitioning in DPPC starts at temperatures corresponding to the polar head pretransition, in agreement with the variation of the 3wGP value reported in Fig. 7. From Fig. 8 (and Table 2) we can observe that at 25°C, the  $R_M$  and  $C_p$  values are lower in the gel with respect to the liquid-crystalline phase by a factor of ~35. Both in the liquid-crystalline phase and in the presence of coexisting phases, Prodan partitioning in the bilayer with respect to the aqueous environment decreases as the temperature increases. To show the maximum range variation, in Table 2 we show a comparison between the  $R_M$  and  $C_p$  values, calculated from Eqs. 6 and 8 and Eq. 12 (lower bound), at 25°C.

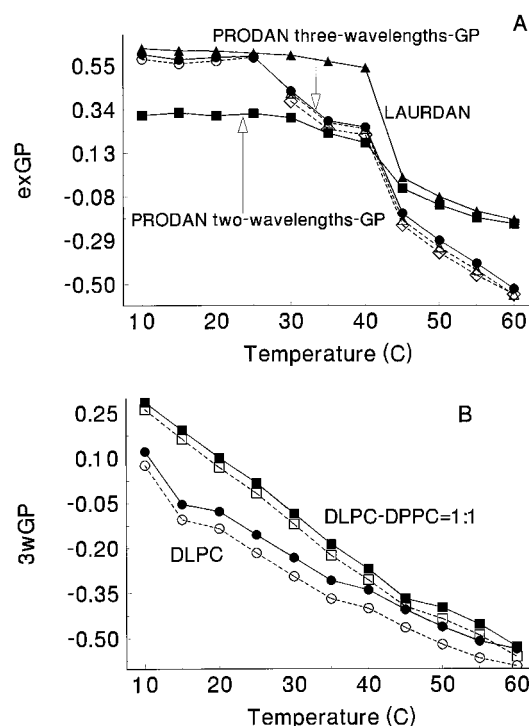


FIGURE 7 (A) Prodan two- (■) and three-wavelength (●, ○, △, ◇) excitation GP in DPPC vesicles as a function of temperature. Laurdan two-wavelength GP (▲) is reported for comparison. The 3wGP values were calculated with Eq. 11 (●) and Eq. 3 with  $R_{31} = 0.081$  (○),  $R_{31} = 0.394$  (△), and  $R_{31} = 0.07$  (◇). (B) Prodan 3wGP in DLPC (●, ○) and in the equimolar mixture of DLPC and DPPC (■, □) as a function of temperature. Values were calculated with the correct Eq. 3 (●, ■) and the simplified Eq. 11 (○, □).

### Excitation and emission 3wGP spectra

Excitation 3wGP spectra have been calculated for the three samples at 25°C, and a comparison with the previously reported two-wavelength GP is shown in Fig. 9. No major differences in the wavelength dependence are observed between the two- and three-wavelength GP spectra obtained in the DLPC and the DLPC-DPPC samples. Instead, in DPPC vesicles, the 3wGP excitation spectrum shows a linear behavior, not dependent on the excitation wavelength, and closely resembling the behavior of the Laurdan GP excitation spectrum obtained in the gel phase (Fig. 2).

TABLE 2 Ratio of PRODAN molecules in membrane and in water,  $R_M$ , PRODAN partition coefficient between membrane and water,  $C_p$ , expressed as  $10^4$  values, and values of the 3wGP obtained at 25°C, in the three phospholipid samples

	$R_M$		$C_p$		3wGP	
	Eqs. 6, 8	Eq. 12	Eqs. 6, 8	Eq. 12	Eq. 3	Eq. 11
DPPC	0.76	0.40	14.09	6.03	0.590	0.610
DLPC	27.26	1.95	504.74	36.19	-0.216	-0.156
1/1 mixture	11.95	9.88	221.22	37.15	-0.017	0.017

From Eqs. 6 and 8 for  $R_M$  and  $C_p$  and Eq. 3 for the 3wGP, and the lower bound simplified Eq. 12 for  $R_M$  and  $C_p$  and Eq. 11 for the 3wGP.

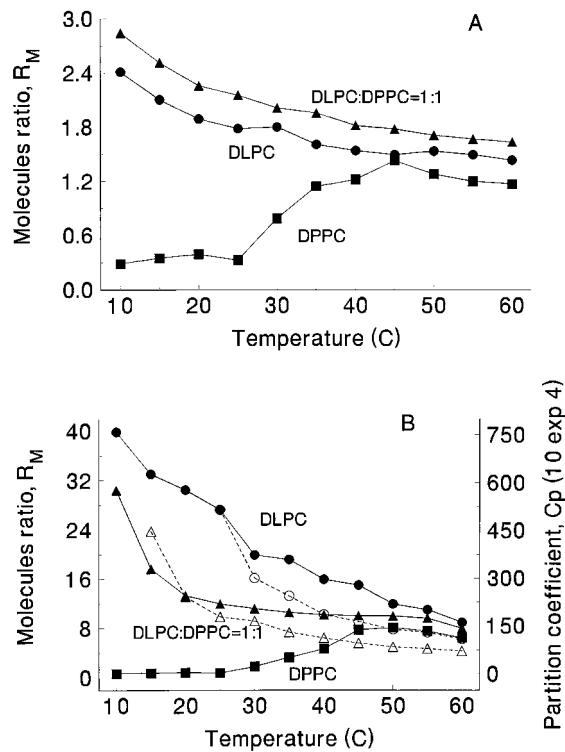


FIGURE 8 Ratio values,  $R_M$ , between Prodan molecules in phospholipids and in water as a function of temperature and values of the partition coefficient,  $C_p$ , between Prodan in phospholipids and in water. (A) Values obtained by using the lower bound of the simplified Eq. 12. (B) Value obtained with the "corrected" Eq. 8, using  $R_{32} = 0.293$ ,  $R_{32} = 0.329$ , and  $R_{32} = 0.405$ , for DPPC, DLPC, and the equimolar mixture, respectively, independent of temperature (○, △, ---), and correcting the  $R_{32}$  values for the temperature variation as reported in the text (●, ■, ▲, —). For the DPPC sample, we used  $R_{32} = 0.293$  from 10°C to 25°C,  $R_{32} = 0.329$  between 30°C and 45°C, and  $R_{32} = 0.405$  between 50°C and 60°C. The  $C_p$  values of the right y axis refer to the filled symbols and are expressed as  $10^4$ .

### Time-resolved emission spectra

To further investigate the spectroscopic origin of the spectral shift of Prodan in the different phases, time-resolved emission spectra have been measured at 25°C in the three

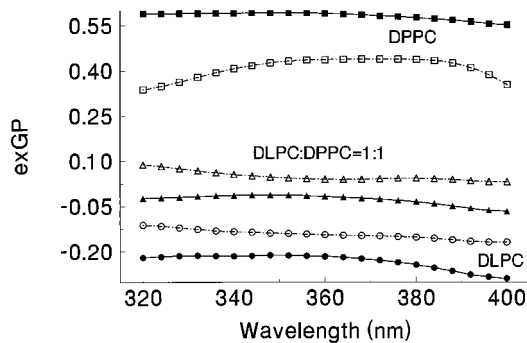


FIGURE 9 Prodan two-wavelength (---) and three-wavelength (—) excitation GP spectra obtained in the phospholipid samples of different phases at 25°C.

phospholipid samples (Fig. 10). The variation of the center of mass of the emission spectra in the three samples as a function of time after excitation is reported in Fig. 11. In DPPC vesicles, where no dipolar relaxation occurs, 20 ns after excitation, the Prodan emission spectrum is still blue (Figs. 10 A and 11). Prodan molecules in water appear as a separate red emission band, already relaxed at very short times after excitation, and rapidly disappearing because of their short lifetime (Table 1). In this last sample, at very short times, we can observe a decrease in the center of mass due to the disappearance of the short component of the decay arising from the emission of Prodan molecules in water. In the DLPC sample, dipolar relaxation results in a continuous redshift of the emission versus time after exci-

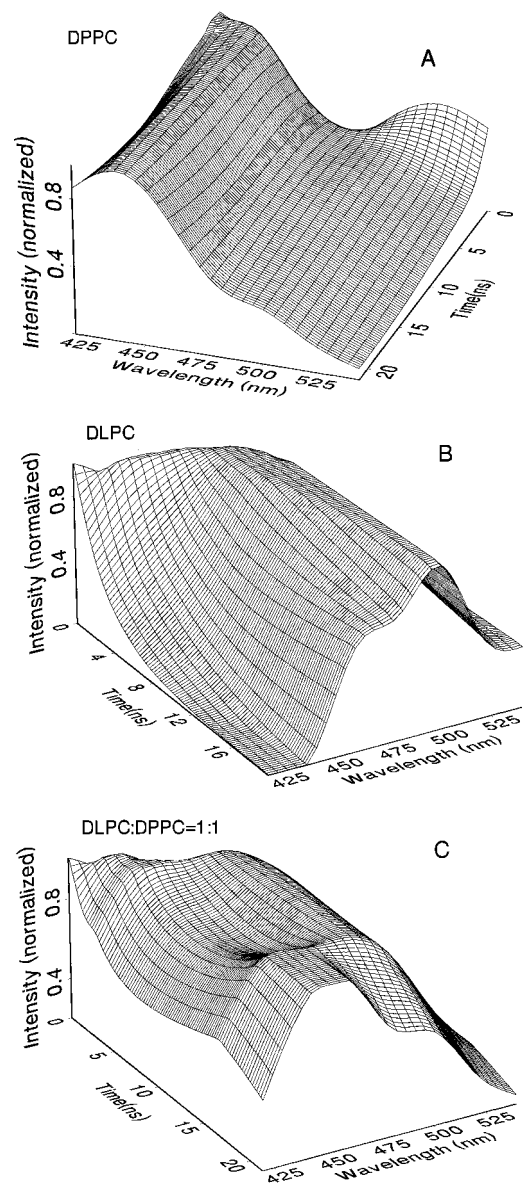


FIGURE 10 Prodan time-resolved emission spectra at 25°C in DPPC (A), DLPC (B), and DLPC:DPPC = 1:1 (C) multilamellar phospholipid vesicles.

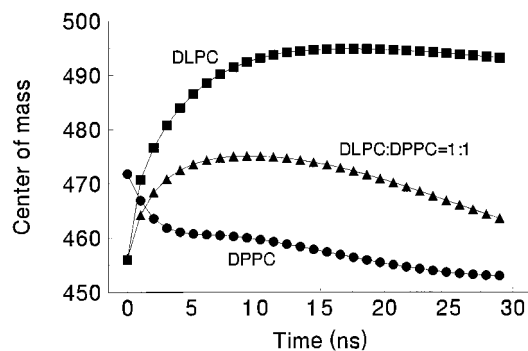


FIGURE 11 Prodan emission center of mass as a function of the time after excitation, calculated from the time-resolved spectra reported in Fig. 10 for the same three samples.

tation (Figs. 10 *B* and 11). In the equimolar mixture of DLPC and DPPC, the emission spectrum shifts toward the red in the first 10 ns after excitation, then is backshifted to the blue (Figs. 10 *C* and 11). This is the characteristic behavior indicative of fluctuation between coexisting phases (Parasassi et al., 1990, 1995).

## DISCUSSION

Like that of Laurdan, the Prodan response to the polarity of the environment can be measured by the steady-state excitation and emission spectra. Because of the higher intensity of the red excitation band, centered at  $\sim 390$  nm, observed in the gel phospholipid phase with respect to the liquid-crystalline phase, a selective excitation of Prodan molecules in the gel phase can be achieved. Moreover, the emission spectra of the probe in the two phospholipid phases are different, showing a redshift of  $\sim 50$  nm in the liquid-crystalline phase. Instead, the generalized polarization (GP), which monitors the extent of the spectral relaxation, can be calculated both for the excitation and for the emission, following procedures similar to those reported for Laurdan (Parasassi et al., 1991a). However, we observed substantial differences in the behavior of the two probes. A relevant result of this work concerns the difference in the Prodan partitioning between the two phospholipid phases. The partition coefficient was determined from the different partition coefficients of the probe between water and each of the two phases. From our determinations, at  $25^\circ\text{C}$  the Prodan partition coefficient between DPPC and water, calculated from Eqs. 6 and 8, is  $C_p = 14 \times 10^4$ , whereas that between DLPC and water is  $504 \times 10^4$ . Thus, in these experimental conditions, it appears that Prodan partitioning is higher in the liquid-crystalline phase by a factor of  $\sim 35$ . As shown in Fig. 8 *B*, this factor is a function of temperature.

The determination of Prodan partition coefficients has been possible because of the attribution of the red emission band to the fluorescence of Prodan molecules in water, and because of the formulation of a procedure to subtract the probe emission in water from its total emission. This band is clearly observable in pure gel phase phospholipids such

as DPPC below  $40^\circ\text{C}$ . We presented a variety of experimental evidence supporting the attribution of this red emission band to the fluorescence of Prodan molecules in water:

1. The dilution experiments proved that there is an appreciable amount of total fluorescence arising from Prodan molecules in water and that, because of Prodan partitioning, by diluting the phospholipids, the probe is extracted by the aqueous phase. The emission spectra collected in the dilution experiments showed a progressive relative increase in the red emission band, attributed to Prodan fluorescence in water, and a decrease in the blue band, attributed to Prodan fluorescence in the phospholipid (Fig. 4).

2. In the DPPC sample, Prodan fluorescence polarization showed an abrupt decrease with the increase of the emission wavelength, reaching a value very close to that measured in water at wavelengths greater than 480 nm.

3. The lifetime measurements gave a double exponential decay for Prodan in DPPC below the transition temperature, with a short lifetime component of about the same as that of the probe in water. With a longer wavelength cutoff filter, the fractional intensity of the short component increased.

4. The time-resolved spectra show the disappearance of the red band a few nanoseconds after excitation (Figs. 10 *A* and 11), a characteristic behavior of a component with a short lifetime. Both the polarization points measured at three different emission wavelengths and the single-frequency lifetime values reported by Zeng and Chong (1991) are in agreement with our results. From the above evidence, the proposed attribution of Prodan emission features to the probe location at various depths along the bilayer (Chong et al., 1989) is unlikely. The emission of Prodan molecules in water cannot be directly observed in the phospholipid liquid-crystalline phase, because the probe emission from water and that from the membrane overlap, because of the dipolar relaxation of the probe in fluid membranes. The attribution of the 520-nm band in the DPPC sample to the probe in water is in agreement with previous reports (Zeng and Chong, 1995), where the Prodan partition coefficient was also calculated by an ultracentrifugation method. However, the probe partition coefficient calculated in this work differs by a factor of  $\sim 5$  from that reported by Zeng and Chong. In their work, at  $20^\circ\text{C}$  the Prodan partition coefficient determined between DPPC and water is  $2.8 \times 10^4$ , and in our determinations, at  $25^\circ\text{C}$ , is  $14 \times 10^4$ . We must observe that the method we used here is simpler than that used by Zeng and Chong and does not require delicate manipulations of the sample, but only spectroscopic analysis. However, our method for determining the partition coefficient can be affected by a relatively large error due to the uncertainty in the  $R_{32}$  evaluation.

With regard to the study of membrane properties, we demonstrated the need to subtract the contribution of Prodan fluorescence in water from the probe fluorescence in the phospholipid environment. The 3wGP can be calculated for this purpose. As previously reported (Zeng and Chong, 1995), the simple ratio between the intensities of the blue band and the red band is affected by the phospholipid/probe



ratio. This is not the case for the 3wGP value, because this method effectively subtracts the Prodan emission from water. We varied the ratio between Prodan and DPPC by a factor of 4, from 1:1000 to 1:4000. Whereas the intensity ratio between 425 nm and 503 nm varied by  $\sim 35\%$ , no variations were observed for the 3wGP, which had a constant value of  $0.590 \pm 0.001$  at  $25^\circ\text{C}$ . By using three wavelengths, the calculation of the ratio between the Prodan fluorescence fractional intensity arising from membrane and from water,  $R_F$ , can be also performed (Eq. 3). Assuming that the lifetime is proportional to the quantum yield, the ratio of Prodan molecules in the phospholipid membrane and in water,  $R_M$ , can be calculated by dividing  $R_F$  by the corresponding lifetime values of the probe in the two environments (Eq. 8). If the absolute concentration of the sample is known, the Prodan partition coefficient,  $C_p$ , between the lipids and water can be calculated (Eq. 9). We show that at all temperatures, Prodan partitioning is higher in the liquid-crystalline than in the gel phase (Fig. 8). For Laurdan, the longer acyl chain prevents this probe from partitioning in water. The loose hydrophobic interaction of Prodan with the bilayer renders this probe particularly sensitive to the packing properties of the membrane surface. Contrary to Laurdan, Prodan molecule appears to be squeezed out from a well-packed, gel phase membrane. The polar head pre-transition allows the increase of Prodan partitioning in the bilayer (Figs. 7 and 8).

Although the contribution of Prodan fluorescence arising from water can be accounted for by the use of the 3wGP, an additional effect exists: in the case of coexisting phospholipid phases, Prodan fluorescence mainly monitors the properties of the liquid-crystalline phase. This conclusion is based both on the partition coefficients determined in the different phases and on the wavelength dependence of the GP spectra. Both emission GP (Fig. 2) and three-wavelength excitation GP (Fig. 9) display a wavelength-dependent behavior, and their slope is a function of the phospholipid phase state. The origin of the wavelength dependence of the GP spectra is in the dipolar relaxation phenomenon, as previously discussed for Laurdan (Parasassi and Gratton, 1995). For Prodan, the wavelength dependence of both emission GP and 3wGP spectra obtained in the equimolar mixture of DLPC and DPPC does not show appreciable differences with respect to the GP spectra obtained in pure DLPC.

Prodan time-resolved emission spectra are consistent with the above discussion. The time-resolved experiments confirmed the attribution of Prodan spectral features to the dipolar relaxation phenomenon. In environments where the dynamics of the dipoles surrounding the fluorescent moiety of Prodan occur on a time scale comparable to that of the Prodan excited state, the solvent dipoles can reorient around the Prodan excited state dipole. The energy required for such a reorientation results in a redshift of the probe emission. In dipolar relaxing environments, such as the liquid-crystalline phase of DLPC vesicles, the emission center of mass shifts toward the red with time after excitation. In

nonrelaxing environments, such as the DPPC vesicles in the gel phase, the emission is unchanged with time. Interestingly and in agreement with results obtained with Laurdan (Parasassi et al., 1990; Parasassi and Gratton, 1995), using Prodan in vesicles composed of an equimolar mixture of the two phases, we can observe a red spectral shift in the first 10 ns after excitation. Then the emission is progressively backshifted toward the blue. The midpoint of such an inversion occurs  $\sim 20$  ns after excitation. This behavior has been interpreted as being representative of the fluctuation between two coexisting phases (Parasassi et al., 1990). By using Prodan, we can still observe such an inversion of the direction of the emission spectral shift, but the dynamics of the phase fluctuation appears to be faster than that measured for Laurdan, this last being  $\sim 30$ – $50$  ns. This may be due to the different location of Prodan, which is closer to the more polar surface of the bilayer, which may fluctuate more rapidly, to the preferential partitioning of Prodan in a more fluid phase, and to the shorter lifetime of Prodan.

The parallel use of Laurdan and Prodan to monitor structural and dynamical changes of membrane properties has been already shown to be advantageous (Parasassi et al., 1994b). The use of the 3wGP, which gives the possibility of calculating the probe partition coefficient between the membrane and water, may render the use of Prodan even more attractive.

This work was supported by CNR (EKK, TP) and by the National Institutes of Health RR03155 (EG).

## REFERENCES

- Bondar, O. P., and E. S. Rowe. 1996. Thermotropic properties of phosphatidylethanolols. *Biophys. J.* 71:1440–1449.
- Chiu, S.-W., M. Clark, V. Balaji, S. Subramanian, H. L. Scott, and E. Jakobsson. 1995. Incorporation of surface tension into molecular dynamics simulation of an interface: a fluid phase lipid bilayer membrane. *Biophys. J.* 69:1230–1245.
- Chong, P. L. 1988. Effects of hydrostatic pressure on the location of Prodan in lipid bilayers and cellular membranes. *Biochemistry.* 27:399–404.
- Chong, P. L., S. Capes, and P. T. T. Wong. 1989. Effect of hydrostatic pressure on the location of Prodan in lipid bilayers: a FT-IR study. *Biochemistry.* 28:8358–8363.
- Damodaran, K. V., and M. M. Kenneth, Jr. 1994. A comparison of DMPC- and DMPE-based lipid bilayers. *Biophys. J.* 66:1076–1087.
- Heller, H., M. Schaefer, and K. Schulten. 1993. Molecular dynamics simulation of a bilayer of 200 lipids in the gel and in the liquid-crystalline phases. *J. Phys. Chem.* 97:8343–8360.
- Huang, Z., and R. Haugland. 1991. Partition coefficients of fluorescent probes with phospholipid membranes. *Biochem. Biophys. Res. Commun.* 181:166–171.
- Lakowicz, J. R., D. R. Bavan, B. P. Maliwal, M. H. Cherek, and A. Balter. 1983. Synthesis and characterization of a fluorescence probe of the phase transition and dynamic properties of membranes. *Biochemistry.* 22:5714–5722.
- MacGregor, R. B., and G. Weber. 1981. Fluorophores in polar media: spectral effects of the Langevin distribution of electrostatic interactions. *Ann. N.Y. Acad. Sci.* 366:140–154.
- Massey, J. B., H. S. She, and H. J. Pownall. 1985. Interfacial properties of model membranes and plasma lipoproteins containing ether lipids. *Biochemistry.* 24:6973–6978.

- Nagle, J. F., and D. A. Wilkinson. 1978. Lecithin bilayers. Density measurements and molecular interactions. *Biophys. J.* 23:159–175.
- Parasassi, T., G. De Stasio, A. d'Ubaldo, and E. Gratton. 1990. Phase fluctuation in phospholipid membranes revealed by Laurdan fluorescence. *Biophys. J.* 57:1179–1186.
- Parasassi, T., G. De Stasio, G. Ravagnan, R. M. Rusch, and E. Gratton. 1991a. Quantitation of lipid phases in phospholipid vesicles by the generalized polarization of Laurdan fluorescence. *Biophys. J.* 60:179–189.
- Parasassi, T., G. De Stasio, R. M. Rusch, and E. Gratton. 1991b. A photophysical model for diphenylhexatriene fluorescence decay in solvents and in phospholipid vesicles. *Biophys. J.* 59:466–475.
- Parasassi, T., M. Di Stefano, M. Loiero, G. Ravagnan, and E. Gratton. 1994a. Influence of cholesterol on phospholipid bilayers phase domains as detected by Laurdan fluorescence. *Biophys. J.* 66:120–132.
- Parasassi, T., A. M. Giusti, E. Gratton, E. Monaco, M. Raimondi, G. Ravagnan, and O. Sapora. 1994b. Evidence for an increase in water concentration in bilayers after oxidative damage of phospholipids induced by ionizing radiation. *Int. J. Radiat. Biol.* 65:329–334.
- Parasassi, T., and E. Gratton. 1995. Membrane lipid domains and dynamics as detected by Laurdan fluorescence. *J. Fluorescence.* 5:59–69.
- Parasassi, T., E. Gratton, W. M. Yu, P. Wilson, and M. Levi. 1997. Two-photon fluorescence microscopy of Laurdan GP domains in model and natural membranes. *Biophys. J.* 72:2413–2429.
- Parasassi, T., M. Loiero, M. Raimondi, G. Ravagnan, and E. Gratton. 1993. Absence of lipid gel-phase domains in seven mammalian cell lines and in four primary cell types. *Biochim. Biophys. Acta.* 1153:143–15.
- Parasassi, T., O. Sapora, A. M. Giusti, G. De Stasio, and G. Ravagnan. 1991c. Alterations in erythrocyte membrane lipids induced by low doses of ionizing radiation as revealed by 1,6-diphenyl-1,3,5-hexatriene fluorescence lifetime. *Int. J. Radiat. Biol.* 59:59–69.
- Rottenberg, H. 1992. Probing the interaction of alcohols with biological membranes with the fluorescent probe Prodan. *Biochemistry.* 31:9473–9481.
- Slavik, J. 1982. Anilinonaphthalene sulfonate as a probe of membrane composition and function. *Biochim. Biophys. Acta.* 694:1–25.
- Stubbs, C. D., C. Ho, and S. J. Slater. 1995. Fluorescence techniques for probing water penetration into lipid bilayers. *J. Fluorescence.* 5:19–28.
- Tang, D., and P. L. Chong. 1992. E/M dips. Evidence for lipids regularly distributed into hexagonal superlattices in pyrene-PC/DMPC binary mixtures at specific concentrations. *Biophys. J.* 63:903–910.
- Virtanen, J. A., M. Ruonala, M. Vauhkonen, and P. Somerharju. 1995. Lateral organization of liquid-crystalline cholesterol-dimyristoylphosphatidylcholine bilayers. Evidence for domains with hexagonal and centered rectangular cholesterol superlattices. *Biochemistry.* 34:11568–11581.
- Weber, G., and F. J. Farris. 1979. Synthesis and spectral properties of a hydrophobic fluorescent probe: 6-propionyl-2-(dimethylamino)naphthalene. *Biochemistry.* 18:3075–3078.
- Zeng, J. W., and P. L. Chong. 1991. Interaction between pressure and ethanol on the formation of interdigitated DPPC liposomes: a study with Prodan fluorescence. *Biochemistry.* 30:9485–9491.
- Zeng, J., and P. L. Chong. 1995. Effect of ethanol-induced lipid interdigitation on the membrane solubility of Prodan, Acдан and Laurdan. *Biophys. J.* 68:567–573.